70-18,512

YOUNG, James Forrest, 1943-
VISIBLE CW OPTICAL PARAMETRIC OSCILLATORS.

Stanford University, Ph.D., 1970
Physics, optics

University Microfilms, Inc., Ann Arbor, Michigan

THIS DISSERTATION HAS BEEN MICROFILMED EXACTLY AS RECEIVED

Reproduced with permission of the copyright owner. Further reproduction prohibited without permission.

VISIBLE CW OPTICAL PARAMETRIC OSCILLATORS

A DISSERTATION

SUBMITTED TO THE DEPARTMENT OF ELECTRICAL ENGINEERING

AND THE COMMITTEE ON THE GRADUATE DIVISION

OF STANFORD UNIVERSITY

IN PARTIAL FULFILLMENT OF THE REQUIREMENTS

FOR THE DEGREE OF

DOCTOR OF PHILOSOPHY

By

James Forrest Young

December 1969

Reproduced with permission of the copyright owner. Further reproduction prohibited without permission.

I certify that I have read this thesis and that in my opinion it is fully adequate, in scope and quality, as a dissertation for the degree of Doctor of Philosophy.

Stephen E Harris
(Principal Adviser)

I certify that I have read this thesis and that in my opinion it is fully adequate, in scope and quality, as a dissertation for the degree of Doctor of Philosophy.

Robert L Byer
(Applied Physics)

I certify that I have read this thesis and that in my opinion it is fully adequate, in scope and quality, as a dissertation for the degree of Doctor of Philosophy.

Robert M. Gray

Approved for the University Committee on the Graduate Division:

Lincoln E Moses
Dean of the Graduate Division

Reproduced with permission of the copyright owner. Further reproduction prohibited without permission.

ABSTRACT

This thesis reports on research directed toward developing cw, tunable, coherent optical sources. One of the main obstacles to successful cw optical parametric oscillators was the lack of high-quality nonlinear materials. The index of refraction inhomogeneities of lithium niobate crystals are described and are explained in terms of the phase diagram of the Li_2O - Nb_2O_5 system. The test procedures and growth techniques which led to high-quality, long crystals are presented.

Using such a crystal the first visible cw optical parametric oscillator was constructed. The oscillator was pumped with the 0.5145 micron multimode power of an argon ion laser and was thermally tuned from 0.68 microns to 0.705 microns at the signal, and 2.11 microns to 1.90 microns at the idler. Both signal and idler waves were resonated. Average signal powers of 3 mW were measured in a 3 cm^{-1} bandwidth. A similar oscillator was built using a three-mirror ring resonator which exhibited improved stability and conversion. An unsuccessful attempt to construct an optical parametric oscillator internal to an argon ion laser using barium sodium niobate is also described.

Reproduced with permission of the copyright owner. Further reproduction prohibited without permission.

ACKNOWLEDGEMENT

Certainly the most important factor in the success of this research was the stimulating environment of the Microwave Laboratory. Excellent physical facilities, great human resources, and a minimum of red tape have been combined in an atmosphere which is warm and relaxed yet filled with the excitement of discovery. I want to thank everyone on the staff of the Laboratory for their help and interest during this work.

Clearly there must be some means of preserving and transmitting results and techniques if a group in which students leave every two or three years is to function. Theoretically, this is the purpose of advisors, lab notebooks, and reports; but every student in our group knows that the true source of such knowledge is Mr. B. Yoshizumi. I want to thank Ben for his excellent technical assistance and good friendship.

My advisor, Professor S. E. Harris, has been a constant source of ideas and encouragement. When everything looked bleak he unfailingly provided a solution or a new direction. I must admit, however, that it is somewhat unnerving to work with someone who produces ideas three times as fast as I can understand them, and ten times as fast as I can do the experiments.

It has been an extremely rewarding experience working with (now) Professor R. L. Byer, both personally and professionally. His enthusiasm and unquenchable optimism carried us through many difficulties.

Reproduced with permission of the copyright owner. Further reproduction prohibited without permission.

The excellent crystals used in this work were grown by R. S. Feigelson at the Center for Materials Research, Stanford University, and fabricated by R. F. Griffin. I want to thank my good friend Suzanne Wise for generally brightening the laboratory and specifically for typing this manuscript. During the course of this work I have been supported by a NASA Traineeship in Optics.

Finally, I would like to thank my parents for their moral and financial support throughout my educational career. Their understanding and interest have been a constant source of encouragement.

Reproduced with permission of the copyright owner. Further reproduction prohibited without permission.

TABLE OF CONTENTS

	Page
Abstract	iii
Acknowledgement	iv
List of Figures	vii
I. INTRODUCTION	1
II. GROWTH OF HIGH QUALITY LITHIUM NIOBATE CRYSTALS	5
Crystal Defects	6
Crystal Growth	7
Crystal Testing and Results	10
III. A VISIBLE CW PARAMETRIC OSCILLATOR	19
Design and Construction	20
Alignment	24
Operating Characteristics	26
IV. FEASIBILITY OF A CW SINGLY RESONANT OSCILLATOR	29
Threshold of a SRO	29
Optical Properties of Barium Sodium Niobate	30
Experimental Results	35
V. A CW RING CAVITY PARAMETRIC OSCILLATOR	37
VI. CONCLUSIONS	42
LIST OF REFERENCES	43

Reproduced with permission of the copyright owner. Further reproduction prohibited without permission.

LIST OF FIGURES

		Page
1.	Phase Diagram of the Li_2O - Nb_2O_5 System from Reference 26	8
2.	Schematic of the Birefringence Test	12
3.	Birefringence Pattern of $LiNbO_3$ Crystals	13
4.	Second Harmonic Power as a Function of Crystal Temperature	18
5.	Schematic of the First CW Visible Optical Parametric Oscillator	23
6.	Parametric Oscillator Average Signal Output Power and Bandwidth as a Function of Input Power	27
7.	Optical Nonlinearity and Half-Wave Voltage of Barium Sodium Niobate as a Function of Crystal Temperature . .	32
8.	Wavelength of Spontaneous Parametric Emission of Barium Sodium Niobate as a Function of Crystal Temperature . .	33
9.	Schematic of the Ring Cavity Optical Parametric Oscillator	39

Reproduced with permission of the copyright owner. Further reproduction prohibited without permission.

CHAPTER I

INTRODUCTION

This thesis reports on research directed toward developing cw, tunable, coherent optical sources. The significant results of this work include the development of long, high quality lithium niobate crystals, construction of the first cw visible optical parametric oscillator, measurement of the properties of barium sodium niobate, and an experimental verification of the properties of a unique three mirror ring cavity cw parametric oscillator. These achievements have been previously reported in the literature by the author in conjunction with other members of the research team (1-4), and this thesis draws heavily from those articles, adding more detail and new data where appropriate.

The physical basis and theory of optical parametric interactions are well known and have been adequately described in the literature. The reader is referred to Harris (5) for a comprehensive review and an extensive bibliography. A brief summary of the historical development of the area, however, may serve to place the current work in perspective, as well as to illustrate the great interest in, and the rapid development of this new field.

The development of the laser in 1960 (6) resulted in an optical source with a greatly increased available optical power per bandwidth per solid angle. Understandably, this factor of 10^6 improvement in the state-of-the-art attracted great attention and opened up a

Reproduced with permission of the copyright owner. Further reproduction prohibited without permission.

multitude of exciting research possibilities. However, it soon became evident that a tunable optical oscillator possessing the coherence, directivity, stability, and monocromaticity of the fixed frequency laser would have even greater usefulness.

The general theory and practical techniques of tunable parametric amplification and oscillation at microwave frequencies were well known (7), and it was proposed (8-10) that similar techniques might be used in the optical region of the spectrum. The physical basis of optical parametric interactions is the small nonlinear polarizability (11) of some non-centrosymmetric crystals which can effect the interchange of energy between optical waves of three different frequencies. The nonlinear polarizability of typical materials is nearly 10^{10} smaller than the first order linear effect and becomes significant only in the presence of the extremely high field strengths obtainable with laser sources. The first practical verification of this nonlinearity was the second harmonic generation of light by Franken, et al. (12) in 1961. The extension of the microwave work into the optical region involved the consideration of a number of new subjects — focusing, double refraction, optical resonators, and phase matching techniques — and the first tunable source was not constructed until 1965 by Giordmaine and Miller (13).

The Giordmaine and Miller oscillator, as well as all subsequent devices, employed a high power Q-switched laser as a pump. The high output powers of these lasers provided the large parametric gains necessary for oscillation, but they suffered from several difficulties.

Reproduced with permission of the copyright owner. Further reproduction prohibited without permission.

The output often varied considerably in power, mode structure, and frequency from pulse to pulse resulting in erratic oscillator operation. In addition, the typical 20 nanosecond pulse length was not long enough to allow the oscillator to reach stable steady-state operation. Consequently, there was considerable interest in constructing an optical oscillator which would exhibit the stability and control of a cw laser. However, the power necessary to achieve sufficient gain for oscillation was far in excess of that available from cw lasers until the discovery of the nonlinear material lithium niobate ($LiNbO_3$) (14). Subsequently, Boyd and Ashkin (15) showed that by using $LiNbO_3$ and by giving proper consideration to correct focusing and to lowering cavity losses, oscillation should be possible using cw lasers. The engineering difficulties of this project may be appreciated by the fact that even with this well defined theory and the experience of the previous pulsed work, almost $2\frac{1}{2}$ years passed before the nearly simultaneous announcement of cw optical parametric oscillators by Smith, et al. (16) at Bell Telephone Laboratories, and Byer, et al. (1) at Stanford University.

One of the main obstacles to developing successful cw oscillators was the lack of suitable nonlinear crystals. Chapter II describes the lithium niobate test procedures and growth techniques which led to the long, high quality crystals necessary for cw oscillators. The construction and operating characteristics of the first cw visible parametric oscillator are given in Chapter III. Chapter IV

Reproduced with permission of the copyright owner. Further reproduction prohibited without permission.

describes an unsuccessful attempt to build a singly resonant cw oscillator using barium sodium niobate. Also included are measurements of the nonlinear optical properties of barium sodium niobate. Chapter V describes a novel cw ring cavity parametric oscillator which combines some of the desirable characteristics of the singly resonant oscillator with the lower threshold of a doubly resonant oscillator. Finally, some brief conclusions are presented in Chapter VI.

Reproduced with permission of the copyright owner. Further reproduction prohibited without permission.

CHAPTER II

GROWTH OF HIGH QUALITY LITHIUM NIOBATE CRYSTALS

The initial announcement (14) of the nonlinear material $LiNbO_3$ created considerable interest for several reasons. The nonlinear polarizability is eleven times greater than KDP. The material is transparent from 0.4μ to 4.5μ . Most importantly, the dispersion and birefringence are such that it is possible to achieve 90° phase matching (17) for many processes of interest with small temperature or electric field perturbations of the indices of refraction. The temperature dependence of the indices of refraction is primarily a result of the ferroelectric nature of the material, and provides a convenient tuning mechanism. Tunable gain was first observed in $LiNbO_3$ using parametric fluorescence (18-19). Early experiments (20), however, indicated that apparently good quality $LiNbO_3$ crystals contained defects which left them useless for nonlinear interactions. We therefore began a lithium niobate development program which ultimately led to the long, high quality crystals necessary for cw parametric oscillators. Our success was in large part due to the excellent facilities of the Center for Materials Research at Stanford University, and in particular to the cooperation and work of R. S. Feigelson of the Center. The principal results of our study are presented below.

Reproduced with permission of the copyright owner. Further reproduction prohibited without permission.

Crystal Defects

The primary defect in $LiNbO_3$ crystals is spatial variations of the birefringence, as first reported by Midwinter (21). Midwinter has also reported (22) that the refractive indices of $LiNbO_3$ are dependent upon crystal composition. Subsequently, there has been further evidence that composition changes are responsible for the observed birefringence variations (23-24). The nonuniform crystal birefringence seriously reduces the efficiency of the nonlinear optical interaction by making it impossible to satisfy the phase matching condition (17) at every point in the crystal, and it is desirable to be able to grow crystals without this defect. These "built-in" index variations due to growth conditions should not be confused with the optically induced damage (25) which can be eliminated by operating above about 160°C .

During growth the crystal composition may change due to a number of factors: temperature fluctuations, preferential loss of one melt constituent due to evaporation, growth rate changes, and melt composition changes due to growth at a non-congruent composition. The variations in crystal composition may occur both in a radial and longitudinal direction. In the following discussion the expected crystal composition variations resulting from changes in growth conditions are compared for growth from congruent and stoichiometric melts.

Reproduced with permission of the copyright owner. Further reproduction prohibited without permission.

Crystal Growth

The crystals used for this study were grown by the Czochralski pulling technique along the a-axis. Details of the apparatus and technique are described elsewhere (4). During the course of testing $LiNbO_3$ crystals grown from melts of various compositions we noticed that melts deficient in Li consistently produced higher quality boules. An examination of the phase diagram of the Nb_2O_5-Li_2O system clarified these results. In interpreting the phase diagram it should be kept in mind that it is taken at equilibrium and is not strictly valid for the dynamic process of crystal growth. However, for the typical slow growth rates it is reasonable to assume that the system is near the equilibrium point. We also assume that no diffusion takes place in the solid, and that complete mixing in the melt takes place due to convective flow.

Recently, the equilibrium phase diagram of the Nb_2O_5-Li_2O system in the vicinity of the $LiNbO_3$ compound has been reconsidered by P. Lerner, C. Legras, and J. P. Dumas (26). Prior to their measurements, the only previous study of the system phase diagram was completed in 1958 by Reisman and Holtzberg (27), but unfortunately was not sufficiently detailed to be useful. Figure 1 is a reproduction of the figure from P. Lerner, et al., showing the phase diagram in the region of $LiNbO_3$ composition, as determined by X-ray and differential thermal analysis techniques. It can be seen that the solid and liquid phases are congruent at a composition of 48.7% $Li_2O/(Nb_2O_5 + Li_2O)$ rather than the stoichiometric 50% concentration. This has

Reproduced with permission of the copyright owner. Further reproduction prohibited without permission.

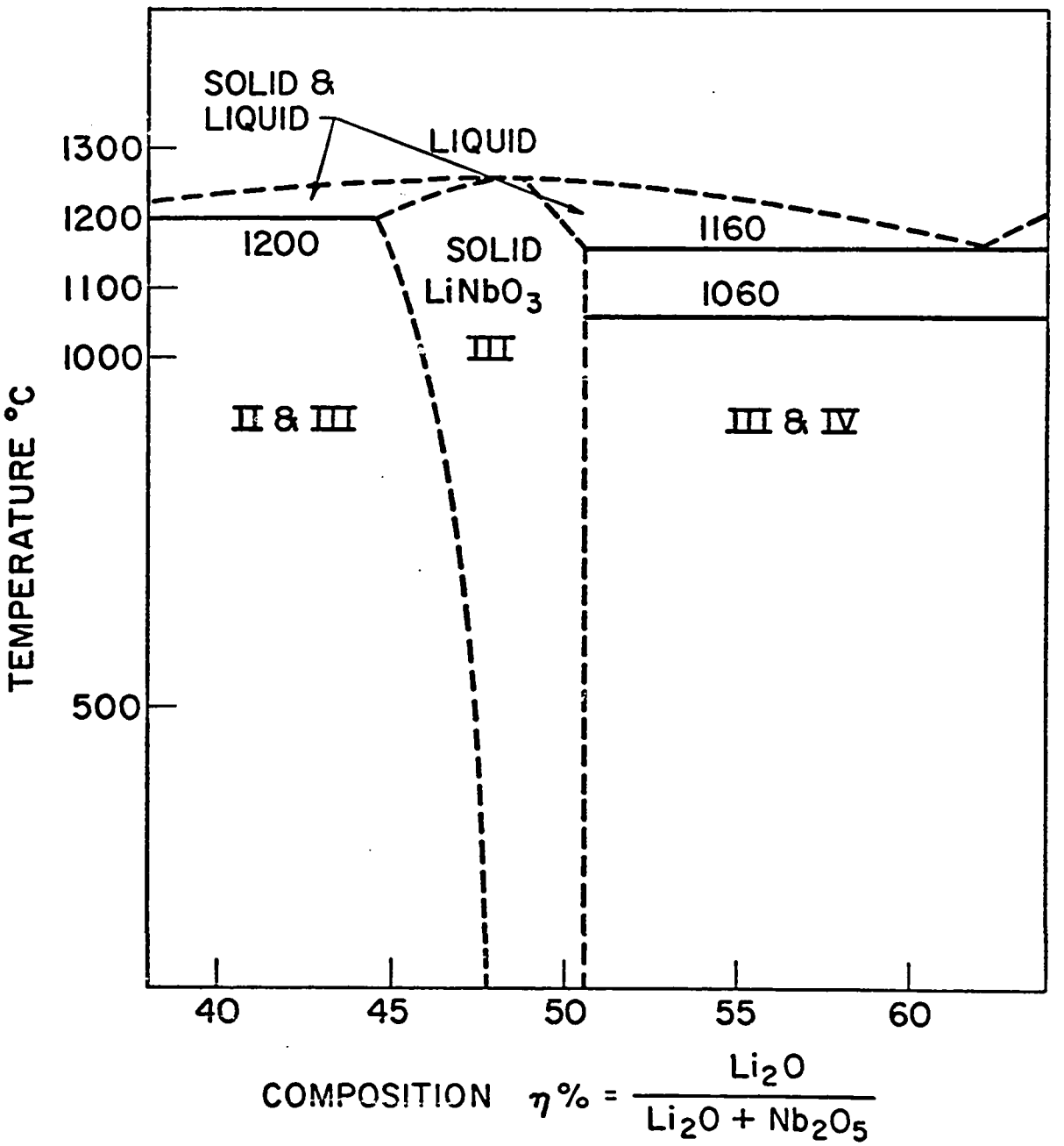

FIG. 1--Phase diagram of the Li_2O - Nb_2O_5 system from Reference 26.

Reproduced with permission of the copyright owner. Further reproduction prohibited without permission.

important results for the composition of $LiNbO_3$ crystals grown from the melt.

Consider first a crystal grown from the stoichiometric melt. The phase diagram indicates that the boule which can exist in equilibrium with the melt has a composition of about 49% Li_2O, rather than 50%. The distribution coefficient k is defined as the ratio of the lithium concentration in the freezing solid C_S, to the concentration in the melt, C_L. In this analysis we consider k to be a constant, having the equilibrium value k_0. Thus as the boule grows the crystal freezes at a composition $C_S = k_0 C_L$. The lithium rejected by the solid enriches the melt and thus both the liquid and solid become progressively lithium richer. Since other evidence (22-24) has shown that the crystal composition directly effects the crystal birefringence, we expect that this will produce a boule with a constantly changing birefringence along the growth direction. Such a linear change has, in fact, been noted by Midwinter (22). Clearly the magnitude of the effect depends upon both k_0 and the fraction g of the liquid that has frozen. This explains the difficulty in growing good large boules and the very poor quality of boules grown from lithium rich melts. Using the known value of k_0 and the dependence of birefringence on composition one can compute a maximum permissable g for crystals which will exhibit 80% theoretical second harmonic conversion efficiency (4). For a stoichiometric melt the boule to melt ratio should not exceed $g \sim 1/25$ for constant birefringence crystals. Obviously a melt large enought to grow long (~ 5 cm) boules would be impractical.

Reproduced with permission of the copyright owner. Further reproduction prohibited without permission.

Growth at melt compositions other than the congruent one also magnifies crystal composition variations due to temperature fluctuations. Temperature fluctuations affect the crystal composition by changing the composition of solid that may exist in equilibrium with the melt. Thus as the boule is grown the fluctuations may cause a composition to freeze at the interface which does not remelt later in equilibrium with the melt. The resulting random birefringence variations can be large and often dominate the linear gradient described above. The magnitude of the composition fluctuations are proportional to temperature through a $(1-k)$ factor, and thus the effect is minimized for congruent growth $(k \simeq 1)$.

It should be clear from the above discussion that these growth problems can be eliminated or considerably reduced by growing from a congruent composition melt. In this case the crystal solidifies at the melt composition and both melt and crystal composition remain constant independent of the fraction solidified. Furthermore, the crystal composition should be relatively independent of small temperature fluctuations as the solid can freeze only at the congruent composition. Thus congruently grown crystals should be of considerably higher quality. The results in the next section confirm that this is indeed the case.

Crystal Testing and Results

Midwinter (21) has described a very useful scheme for observing birefringence gradients directly. The general arrangement is shown

Reproduced with permission of the copyright owner. Further reproduction prohibited without permission.

in Fig. 2. An incident 6328 Å beam polarized 45° to the optic axis excites both an ordinary and an extraordinary wave in the crystal which suffer a relative phase shift proportional to the path length and birefringence at each point in the plane normal to the beam. The resulting elliptically polarized light is analyzed to produce a field with intensity variations corresponding to birefringence changes. To make the birefringence analysis more interpretable it is advantageous to polish the crystal faces with a slight wedge. The crystal then appears with dark bands corresponding to contours of equal birefringence running perpendicular to the plane of the wedge angle. It is then easy to see the small variations in spacing and direction of the fringes which indicate birefringence inhomogeneities. For a crystal of nominally 5 × 5 mm by ℓ in length, a wedge angle of about ten minutes will produce two fringes. The surface flatness requirement is reduced by the birefringence factor $(n_o - n_e)$ so that 1 wave surface flatness is sufficient for this test. Thus the crystals can be prepared quickly and inexpensively. All our $LiNbO_3$ crystals were grown along the a-axis and the crystal orientation shown in Fig. 2 displays the spatial distribution of birefringence variations along the growth direction. This information is very helpful in identifying growth parameters responsible for inhomogeneities and can provide a guide for cutting a good region out of an otherwise bad boule.

Figure 3 shows typical birefringence patterns of crystals grown from stoichiometric and congruent composition melts. The stoichiometric crystal has large random birefringence variations along the

Reproduced with permission of the copyright owner. Further reproduction prohibited without permission.

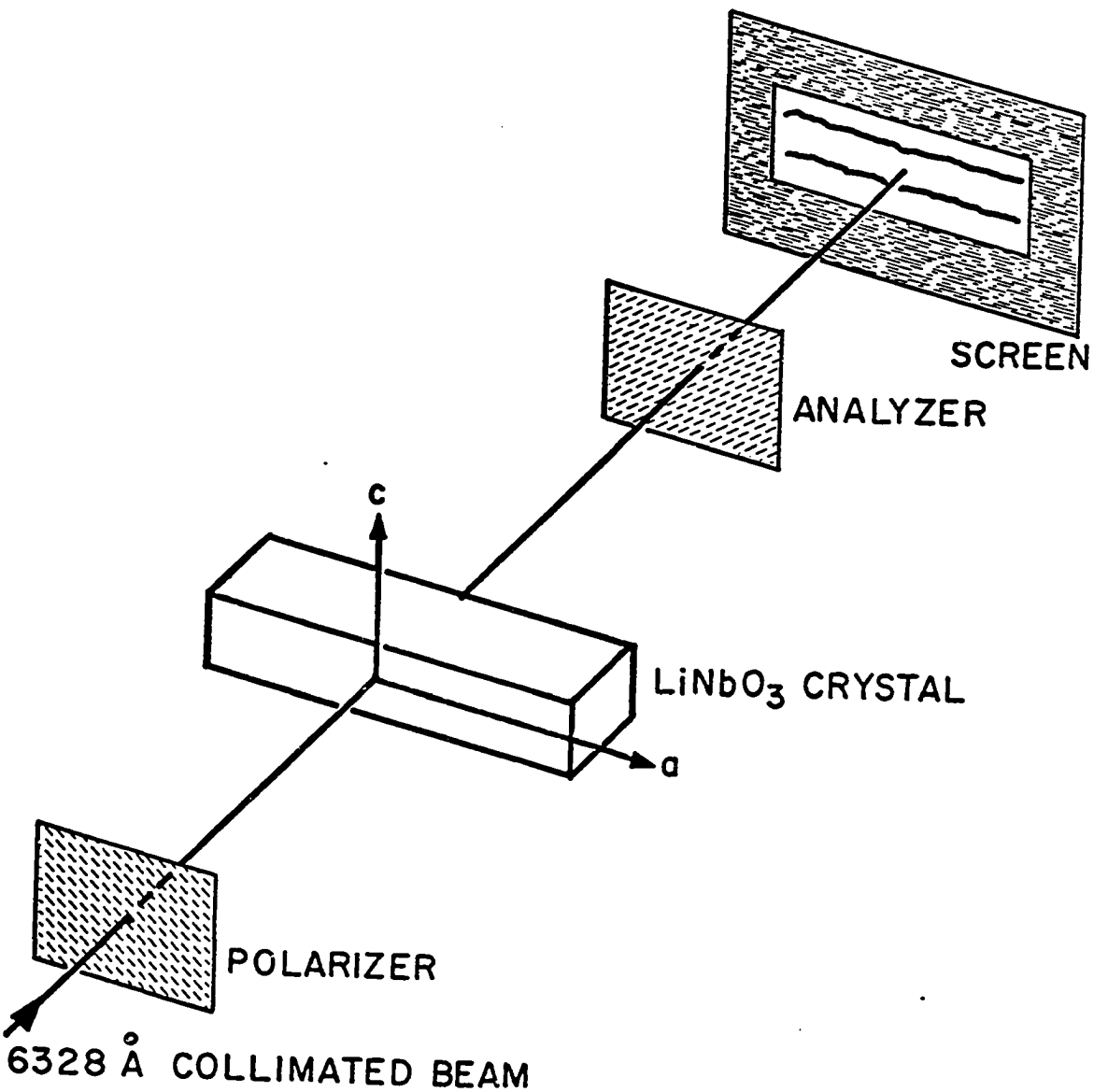

FIG. 2--Schematic of the birefringence test.

Reproduced with permission of the copyright owner. Further reproduction prohibited without permission.

(a)

(b)

FIG. 3--Birefringence pattern of $LiNbO_3$ crystals:
(a) Stoichiometrically grown;
(b) Congruently grown.

Reproduced with permission of the copyright owner. Further reproduction prohibited without permission.

growth direction. These probably result from small temperature variations at the growth interface during growth. The resulting inhomogeneity leaves this crystal useless for phase matched interactions. The congruent crystal was grown under the same conditions but is virtually free of birefringence variations. These are typical results and have been repeated in a large number of boules grown over the period of a year.

Although the birefringence test is useful for qualitatively determining the degree and distribution of inhomogeneities, a simple calculation shows that the minimum observable birefringence variation is several times that tolerated by typical nonlinear processes. For example it can be shown that for 80% theoretical second harmonic generation (SHG) efficiency in a $LiNbO_3$ crystal of length ℓ , the maximum allowed change in birefringence is

$$(n_o^{\omega} - n_e^{2\omega}) = \frac{\lambda_{2\omega}}{4\ell} \quad , \tag{1}$$

where $\lambda_{2\omega}$ is the SH wavelength, and n_o^{ω} and $n_e^{2\omega}$ are the ordinary and extraordinary indices of refraction at the fundamental and SH wavelengths, respectively. We can compare the sensitivity of the birefringence test to the SHG requirements by finding the fractional birefringence fringe shift, δ , produced by the above tolerance. For a crystal of thickness t and length ℓ this fringe shift is

$$\delta = \left(\frac{\lambda_{2\omega}}{\lambda_B}\right) \frac{t}{4\ell} \quad , \tag{2}$$

Reproduced with permission of the copyright owner. Further reproduction prohibited without permission.

where λ_B is the birefringence test wavelength. Assuming $\lambda_{2\omega} \approx \lambda_B$, and a crystal of dimensions $\ell = 20$ mm, t = 4 mm, the fringe shift is of the order of $\delta = 0.05$. In practice, the resolution of the birefringence test is only about 0.25 fringe. Therefore a more sensitive test must be used as a final check of crystal quality.

Clearly the most meaningful test would be to measure the crystal's ability to support a nonlinear interaction. We have found the temperature tuned SHG test suggested by Oshman (20) to provide a convenient, quantitative measure of crystal quality. The general experimental apparatus is well known and has been described elsewhere (22). For propagation perpendicular to the optic axis and near field focusing, the SH power is proportional to the phase mismatch:

$$P_{2\omega} \propto \operatorname{sinc}^2 \left(\frac{\Delta k \ell}{2}\right) , \qquad (3)$$

where ℓ is the interaction length and the wave vector mismatch factor is given by

$$\begin{aligned} \Delta k &= 2k_{\omega} - k_{2\omega} \\ &= \frac{2\pi}{\lambda_{2\omega}} (n_o^{\omega} - n_e^{2\omega}) \quad . \end{aligned} \qquad (4)$$

By expanding the indices of refraction as a function of temperature it is readily shown that the ideal width of the central peak of a SH

Reproduced with permission of the copyright owner. Further reproduction prohibited without permission.

power versus temperature curve is

$$\Delta T \text{ (full width at half maximum)} = \frac{0.89\,\lambda_{2\omega}}{\ell \left| \left(\frac{\partial n_o^{\omega}}{\partial T} - \frac{\partial n_e^{2\omega}}{\partial T} \right)_{T_0} \right|} \quad , \quad (5)$$

where T is temperature and the derivatives are evaluated at the phase matching temperature T_0 . Table I gives values of ΔT , T_0 , and the derivatives for three wavelengths of interest.

TABLE I

Pump Wavelength	$\left(\frac{\partial n_o^{\omega}}{\partial T}\right)_{T_0}$	$\left(\frac{\partial n_e^{2\omega}}{\partial T}\right)_{T_0}$	T_0 (Stoichiometric)	T_0 (Congruent)	ΔT
1.064 μ Nd:YAlG	0.24×10^{-5}	6.08×10^{-5}	47°C	- 8°C	0.81°C
1.084 μ He-Ne	0.27×10^{-5}	6.88×10^{-5}	92°C	42°C	0.73°C
1.152 μ He-Ne	0.29×10^{-5}	8.35×10^{-5}	210°C	172°C	0.64°C

All values except T_0 (congruent) were computed from the data of Hobden and Warner (28), and apply to stoichiometricly grown $LiNbO_3$. The congruent phase matching temperatures given in Table I have been determined experimentally. These experiments also indicated that the calculated values of ΔT also apply to congruent crystals despite

Reproduced with permission of the copyright owner. Further reproduction prohibited without permission.

the shift in T_0 . By computing the ratio of the theoretical and observed values of ΔT one can determine the effective phase-matchable length without having to measure an absolute SH conversion efficiency:

$$\ell_{eff} = \frac{\Delta T_{theory}}{\Delta T_{measured}} \quad . \tag{6}$$

Figure 4 shows the SHG profile of the same two crystals shown in Fig. 3. These tests were made using the He-Ne 1.1523μ line. The superior quality of the congruent crystal is apparent. (The small peak just above the main lobe is believed to be SHG of the low power 1.1525μ line also present in the He-Ne laser). The stoichiometric crystal is so poor that an effective length has little meaning, while the effective length of the congruent crystal is nearly equal to its physical length (38 mm versus 39 mm).

These results illustrate the dramatic improvement in $LiNbO_3$ crystal quality achieved during the course of this work. Presently high quality crystals in excess of 4 cm long can be grown repeatably from congruent melts. Without such crystals the cw parametric oscillators to be described could not have been constructed.

Reproduced with permission of the copyright owner. Further reproduction prohibited without permission.

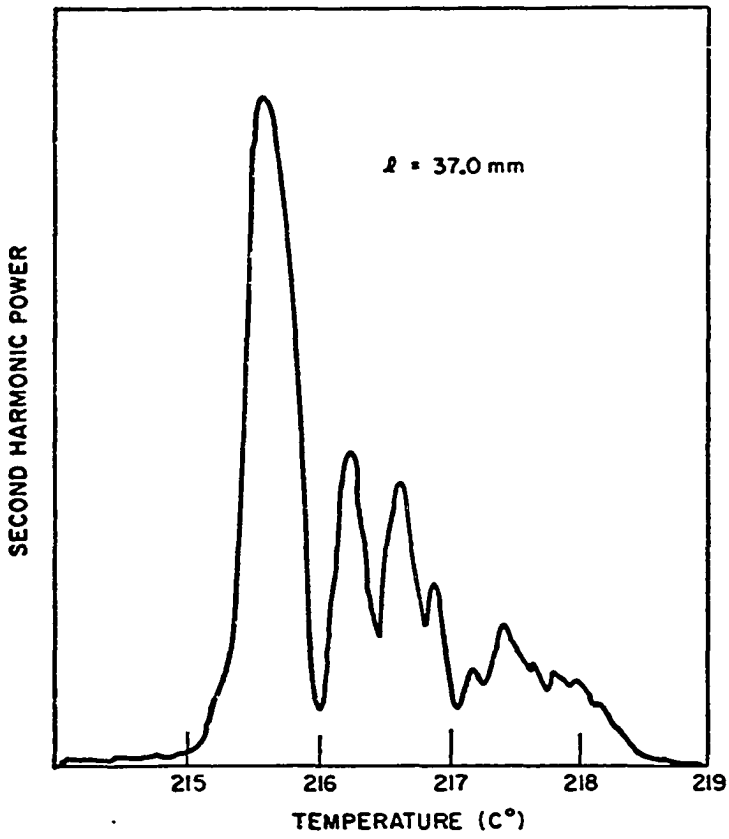

(a)

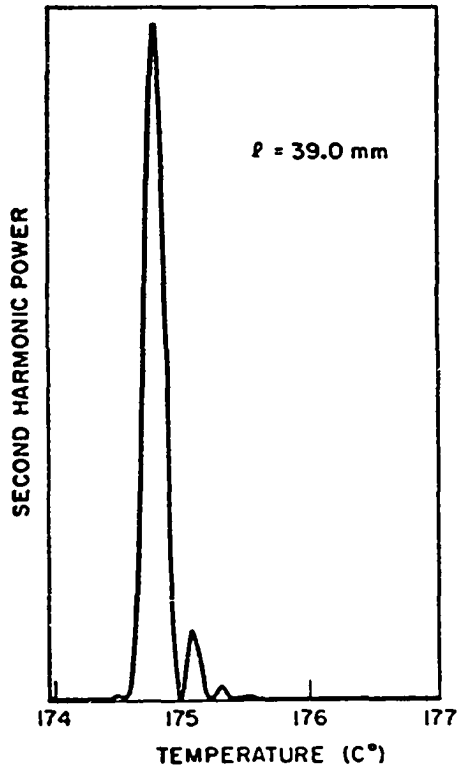

(b)

FIG. 4--Second harmonic power as a function of crystal temperature: (a) Stoichiometrically grown; (b) Congurently grown.

Reproduced with permission of the copyright owner. Further reproduction prohibited without permission.

CHAPTER III

A VISIBLE CW PARAMETRIC OSCILLATOR

In simplest terms there are only two requirements for optical parametric oscillation: intense pump fields within a nonlinear material to create gain, and some means of providing positive feedback to the resulting amplifier. A number of possible schemes for achieving these conditions have been proposed. The effectiveness of the available pump power may be enhanced by placing the nonlinear crystal within an optical cavity resonant at the pumping wavelength, by placing the crystal inside the laser resonator (internal oscillator) (29), by mode locking the pumping laser (30), or by making use of all the available longitudinal laser modes (31). Optical resonators can be used to supply feedback at both the parametric signal and idler frequencies, or at only one of the two. Although the doubly resonant oscillator (DRO) has the lower gain threshold for oscillation because of the greater energy feedback provided, the dual boundary conditions create a number of problems. The mirrors of the oscillator cavity must be highly reflecting at two distinct frequencies and generally have a narrow bandwidth. In addition, oscillation is possible only at signal and idler frequencies which simultaneously are modes of the resonator, and which satisfy the energy conservation condition of the parametric interaction, $\nu_s + \nu_i = \nu_p$. As a result of dispersion the axial mode spacing

Reproduced with permission of the copyright owner. Further reproduction prohibited without permission.

of the signal and idler frequencies are different and the particular modes which satisfy the above requirements may lie outside the parametric gain bandwidth. The frequencies of these "clusters" (13) of allowed modes is very sensitive to temperature changes, mechanical vibration of mirrors, and laser frequency shifts. As a result the oscillator output is quite erratic with regard to frequency and time. Finally, Siegman (32) pointed out that a DRO has limited conversion efficiency because as the resonating signal and idler pass through the nonlinear element in the backward direction (with respect to the input pump) they are phase matched for a sum generation process. The resulting backward wave at the pump frequency removes energy from the process, limits the efficiency, and travels directly back into the pumping laser causing severe frequency and mode instabilities. All these problems are eliminated in a singly resonant oscillator (SRO), but the higher threshold is significantly above the capabilities of available cw pump sources. Therefore, a DRO was constructed as an initial, proof-of-theory experiment.

Design and Construction

The parametric oscillator used lithium niobate as the nonlinear crystal and the cw output of an argon ion laser (5145 Å) as the pump. The signal wavelength was tunable from 6800 Å to 7050 Å with the idler in the corresponding range 2.11μ to 1.90μ . Essential to the operation of the oscillator was the use of the full multimode power of the laser in pumping the oscillator. In addition, operation far from the

Reproduced with permission of the copyright owner. Further reproduction prohibited without permission.

degenerate condition $\nu_s = \nu_i$, and use of a relatively long crystal resulted in measured bandwidths of oscillation about ten times less than those previously reported. A cw-pumped parametric oscillator has been reported by Smith, et al. (16). Smith's oscillator used barium sodium niobate as the nonlinear material, and operated near degeneracy in the IR, with a large bandwidth. In contrast to all previous oscillators which used short optical cavities, our oscillator was constructed with a long cavity to allow for the full use of the multi-frequency pump. The separation of the oscillator mirrors was arranged so that the $c/2L$ frequency spacing of the idler modes was equal to the $c/2L$ frequency spacing of the pumping laser. As shown by Harris (31), this condition allows the comb of pump modes to cumulatively drive a single signal mode by interacting with the comb of equally spaced idler modes. Although the pump modes may be randomly phased and erratic in amplitude due to competition effects in the laser, corresponding behavior of the idler modes should compensate to allow continuous pumping of a single signal mode.

The $LiNbO_3$ crystal was 1.65 cm long. Second harmonic generation experiments established that the crystal did not exhibit significant refractive index inhomogeneities. The particular wavelengths of the signal and idler allow phase matching at elevated temperatures (nominally 240°C for this particular crystal) and thus avoided optically induced refractive index inhomogeneities. Earlier attempts to construct a cw oscillator using the 4880 Å argon ion laser line failed, apparently because of the inhomogeneities

Reproduced with permission of the copyright owner. Further reproduction prohibited without permission.

produced at the lower (150°C) phase matching temperature. More importantly, however, this particular three-to-one ratio of wavelengths simplifies the fabrication of dual wavelength mirrors and antireflection coatings since a quarter-wave coating at the idler wavelength represents a three-quarter wave coating at the signal wavelength. However, the narrow-band nature of the coatings in the third order limited the tuning range of the signal to about 300 Å.

A schematic of the parametric oscillator cavity is shown in Fig. 5. The internal collimating lens is necessary to maintain small signal and idler spot sizes at the output mirror of such a long optical cavity. The additional loss added by the lens is somewhat offset by its easing of cavity length tolerances associated with a tight focus. For example, a hemispherical cavity of this length would have to be operated within 0.003 cm of its instability point to produce an equivalent focus. Because of the lens' demagnification of the longitudinal displacement of the flat mirror, the length of our cavity could be adjusted over several cm with little effect. The lens surface also provided a useful screen for observing the cavity mode pattern and reflections from other components during alignment. This cavity was designed with the aid of a computer program (33) based on the ray matrix calculations described by Kogelnick and Lee (34).

For the spacings shown in Fig. 5, the signal and idler beam waists are located at the center of the crystal with calculated radii of 34μ and 67μ, respectively. The pump was mode matched

Reproduced with permission of the copyright owner. Further reproduction prohibited without permission.

Reproduced with permission of the copyright owner. Further reproduction prohibited without permission.

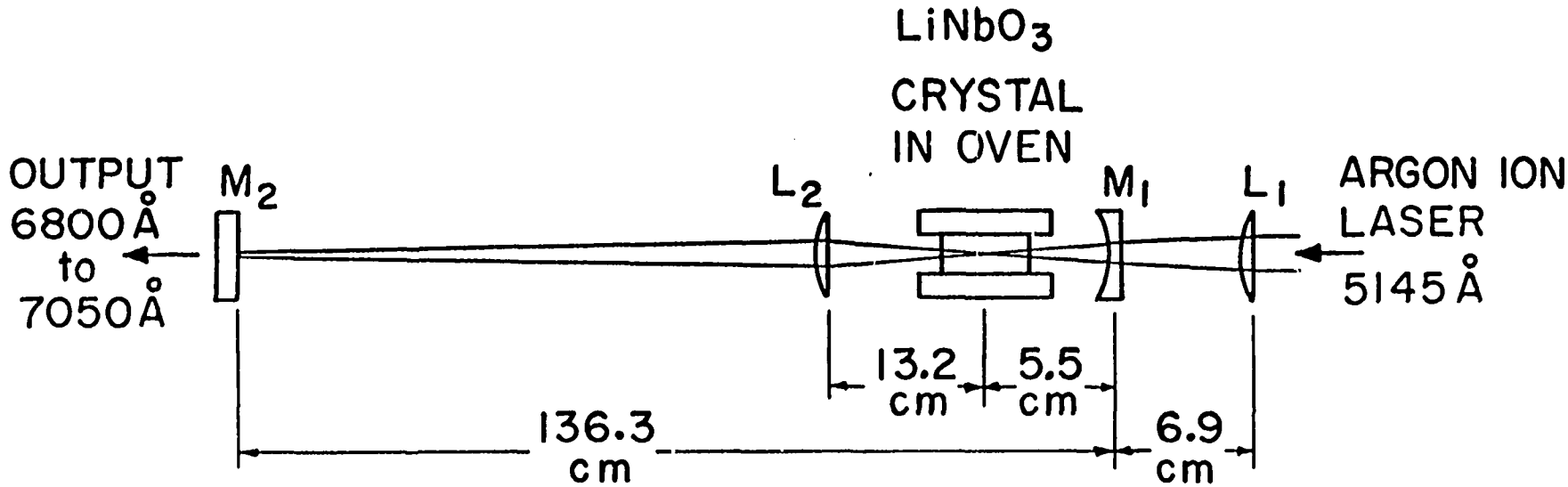

M_1 5cm RADIUS MIRROR

M_2 FLAT MIRROR

L_1 MATCHING LENS, FOCAL LENGTH 9.8cm (5145Å)

L_2 COLLIMATING LENS, FOCAL LENGTH 11.8cm (6900Å)

FIG. 5--Schematic of the first cw visible optical parametric oscillator.

into the parametric cavity and had a beam waist of 29μ . The measured single-pass power losses due to scatter and reflection losses at component surfaces were 5.4% and 2.0% at the signal and idler wavelengths, respectively. For these beam sizes and losses, the results of Boyd and Ashkin (15) predict a single-mode threshold power of approximately 530 mW .

Alignment

Realization of theoretical threshold depends critically on cavity alignment. Alignment of the oscillator is considerably more difficult than alignment of a typical interferometer cavity. In addition to aligning the oscillator resonator components, the cavity as a whole must be aligned strictly collinear with the pump beam. The ~ 30μ radius cavity and pump focal regions must overlap over the entire crystal length to within a fraction of their radii in order to achieve the theoretical gains. The major practical and psychological problem is that, because the oscillator is a threshold device, there is no way to measure the degree of alignment and to make systematic adjustments before threshold is reached. Consequently, many hours were spent adjusting alignment and looking for oscillation without knowing if we were very close to alignment, perfectly aligned but with insufficient pump power, or extremely misaligned with no possibility of oscillation. This uncertainity was finally eliminated by placing a He-Xe rf-excited plasma tube inside the oscillator cavity between the lens and flat mirror.

Reproduced with permission of the copyright owner. Further reproduction prohibited without permission.

The He-Xe plasma has a very high gain line at 3.5μ , and a lower gain line at 2.026μ . After the initial alignment with the pump beam, oscillation could always be obtained at 3.5μ . Cavity alignment could then be improved monitoring the 3.5μ power, until finally the 2.026μ line would oscillate within the cavity. Then the $LiNbO_3$ crystal was temperature tuned to phase match difference frequency generation between the 5145 Å pump and the 2.026μ oscillation. The resulting output at 6896 Å provided a very sensitive measure of both the cavity alignment and beam overlap within the nonlinear crystal. Careful optimization of alignment resulted in a factor of 300 improvement in the power generated at 6896 Å . Finally, the He-Xe plasma tube was removed and small mirror "wiggling" produced oscillation. The measured threshold was 410 mW .

Following the initial alignment the oscillator proved to be quite reliable and tolerant. The crystal and the mirrors could be removed for cleaning and replaced with only minor alignment changes. Alignment techniques using the mode spots on the cavity lens were developed which, with experience and practice, were sufficient to obtain oscillation. The oscillator was completely disassembled and reconstructed successfully on two occasions without the aid of the He-Xe plasma tube. To the eye the oscillator output looked like a deep red He-Ne laser beam, including the sparkling appearance characteristic of coherent light sources. The colorful spectacle of green light changing to red within a small crystal continued to fascinate everyone associated with it long after the initial excitement had worn off.

Reproduced with permission of the copyright owner. Further reproduction prohibited without permission.

Operating Characteristics

Observation of the beat spectrum of the laser output verified the erratic, multimode nature of the pump which, together with the threshold results, confirmed the fact that the full multimode power of the laser was useful in pumping the oscillator. The results of measurements of the output power of the oscillator are shown in Fig. 6. A maximum output power of 1.5 mW as measured with a thermopile was observed when the pumping power was 2.8 times the threshold value. Subsequent improvements in cavity stability and pump power resulted in a 3 mW output. The output mirror of the oscillator has a transmission of only 0.04% and it is expected that larger powers could be obtained with more optimum output coupling. The parametric output consists of pulses with lengths typically 0.1 msec long but occasionally lasting 1 msec . The oscillator wavelength can be continuously tuned by changing the temperature of the crystal. The oscillator maintains nearly constant output power during the tuning process.

Measurements of the spectrum of the oscillator were made with a scanning Fabry-Perot etalon. With an etalon spacing of 1.0 mm corresponding to a free spectral range of 5.0 cm^{-1} , it was found that the total oscillation width (i.e., the bandwidth over which individual cavity modes can oscillate) approaches 3 cm^{-1} if the oscillator is driven reasonably far above threshold. For weaker pump drives this bandwidth is reduced, as shown in Fig. 6. The maximum oscillation

Reproduced with permission of the copyright owner. Further reproduction prohibited without permission.

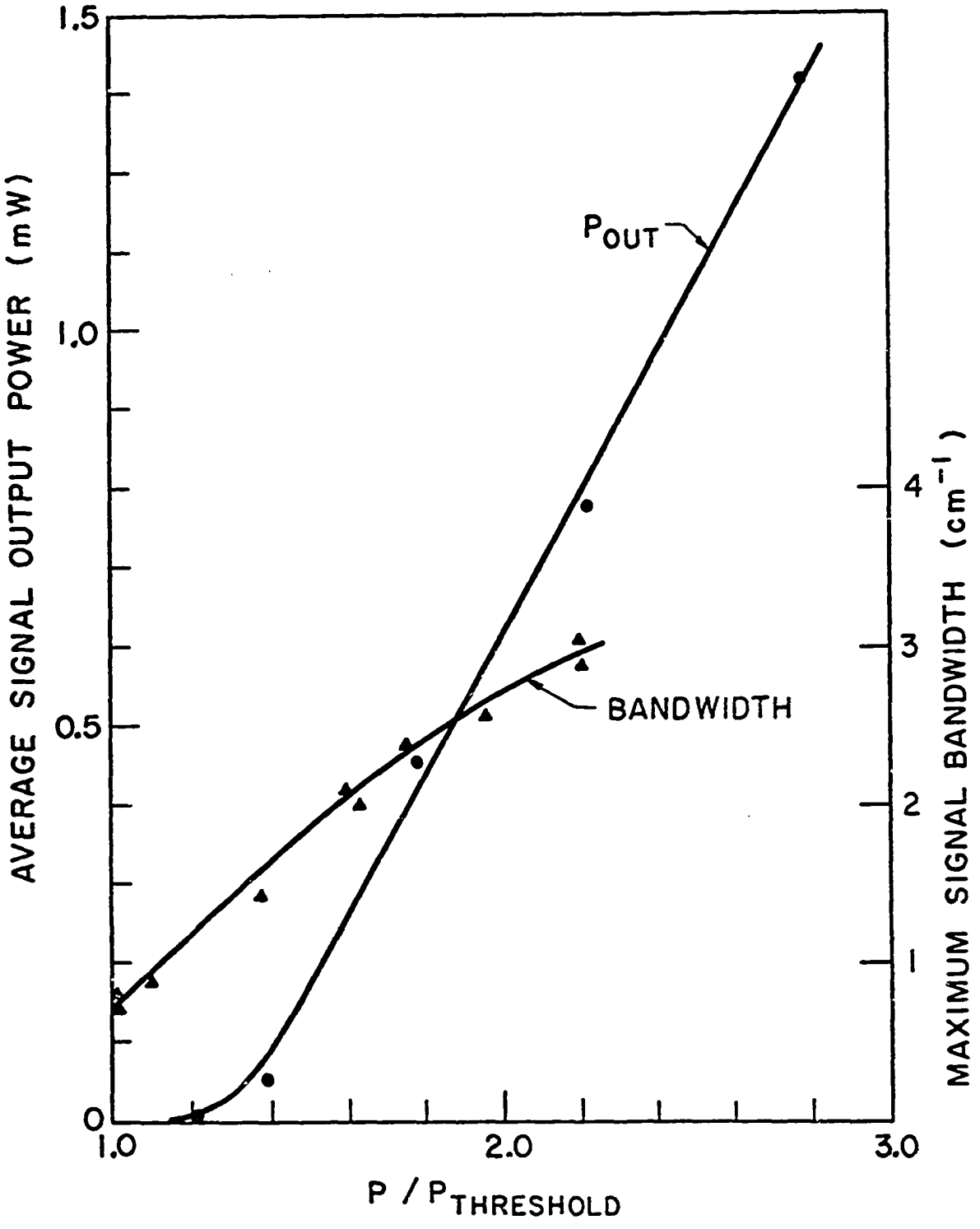

FIG. 6--Parametric oscillator average signal output power and bandwidth as a function of input power.

Reproduced with permission of the copyright owner. Further reproduction prohibited without permission.

width of 3 cm^{-1} is in good agreement with the minimum spontaneous emission bandwidth of $0.886/b\ell = 4.0\ cm^{-1}$ where

$$b = \frac{\partial k_s}{\partial \nu_s} - \frac{\partial k_i}{\partial \nu_i} \quad ,$$

and ℓ is the length of the nonlinear crystal (19).

A Spectra-Physics confocal etalon with a free spectral range of about 3 GHz was used to examine the output spectrum in finer detail. The signal tended to oscillate in a single axial mode at a time, although occasionally two or more modes were observed simultaneously. Erratic signal beat notes at $c/2L$, $2c/2L$, and $3c/2L$ were occasionally observed on a rf spectrum analyzer.

The erratic behavior of this oscillator left much to be desired. However, it verified the theory and provided the experience and confidence necessary to attempt more advanced designs.

Reproduced with permission of the copyright owner. Further reproduction prohibited without permission.

CHAPTER IV

FEASIBILITY OF A CW SINGLY RESONANT OSCILLATOR

Threshold of a SRO

Following the success of the cw DRO described in Chapter III we considered the possibility of constructing a cw SRO. Elimination of the resonator boundary conditions for one of the parametrically generated waves also eliminates the mirror problems, cluster effect, and limited efficiency of the DRO, but only at the cost of a considerably increased threshold. The threshold of a SRO can be estimated quickly by multiplying the equivalent DRO threshold by $2/\alpha$, where α is the loss of the wave which is to be left free. For example, converting the previous DRO into a SRO by eliminating the idler resonance ($\alpha = .02$) would increase the pump power threshold from 0.41 watts to 41 watts. Use of simpler, single wavelength coatings would probably reduce the signal loss by a factor of two, reducing the threshold to about 20 watts. This is still far in excess of cw laser output powers. However, the circulating power within a laser cavity can be quite high. Typically, an argon ion laser provides 1 watt of power at 5145 Å through a 6% transmitting mirror, indicating an internal power of about 16 watts. The 6% coupling loss is probably only slightly greater than the laser should suffer from the internal $LiNbO_3$ crystal due to bulk absorption (2.5%/cm) and scattering loss. Thus the internal SRO experiment appears to be too marginal to be practical.

Reproduced with permission of the copyright owner. Further reproduction prohibited without permission.

In 1967 Geusic, et al. (35) reported the existance of large optical nonlinear coefficients (~ 3 times $LiNbO_3$) in the material barium sodium niobate ($Ba_2NaNb_5O_{15}$); and Smith, et al. (16) used this material to attain low threshold cw optical parametric oscillation. Use of this higher gain material could lower the SRO threshold to a practical value, and we began an investigation of its properties.

Optical Properties of Barium Sodium Niobate

Barium sodium niobate undergoes a crystal structure change at about 300°C . Below this transition temperature the crystal is orthorhombic, biaxial, and generally composed of small microcrystals or twins. Adjacent microcrystals have their c-axes parallel, but have their a and b axes interchanged. A detwinning procedure has been described (35), but has not proved completely satisfactory. For this reason we were particularly interested in the properties of $Ba_2NaNb_5O_{15}$ between 300° and 560°C , where it exists in a ferroelectric tetragonal phase. In this region, the crystal is uniaxial, does not require detwinning, and is of higher optical quality than below 300°C . Also, since the half-wave voltage is considerably lower than at room temperature it should be possible to achieve significant electro-optic tuning of optical parametric oscillators. Some measurements in the tetragonal phase have been reported by Singh, et al. (36).

The variation with temperature of the nonlinear coefficient $d_{15} = d_{31}$ was determined by SHG with a continuously pumped 1.06μ Nd:YAG laser. The second harmonic power was recorded while continuously

Reproduced with permission of the copyright owner. Further reproduction prohibited without permission.

scanning the crystal temperature from room temperature to 600°C , producing the characteristic $(\sin x/x)^2$ curve. As the temperature was raised from room temperature, the peak height of the side lobes built up and reached a maximum at the phase-matching temperature of 116°C . About 25 peaks of the second harmonic intensity were observed between 40° and 116°C , and 320 peaks with successively declining amplitudes were observed from there to 580°C . The relative magnitude of d^2 was calculated by noting that the ratio of the second harmonic power generated at the peak of the n^{th} side lobe to that generated at the phase-matching temperature is given by

$$(d^2/d_0^2)/[(n + \tfrac{1}{2})\,\pi]^2 \quad ,$$

where d is the magnitude of the optical nonlinearity at the temperature of the n^{th} side lobe, d_0 is its magnitude at the phase-matching temperature, and $n \geq 1$. As shown in Fig. 7, the nonlinearity is constant from room temperature to about 300°C , and then breaks sharply and decreases to zero at the Curie temperature of ~ 560°C .

The half-wave voltage at 6328 Å as a function of temperature is also shown in Fig. 7. The data were taken by applying an electric field along the c-axis and measuring the voltage necessary to cause a shift of one fringe for light propagating down the a-axis.

The potential tuning curves for an argon-pumped $Ba_2NaNb_5O_{15}$ parametric oscillator are shown in Fig. 8. The data was taken by

Reproduced with permission of the copyright owner. Further reproduction prohibited without permission.

Reproduced with permission of the copyright owner. Further reproduction prohibited without permission.

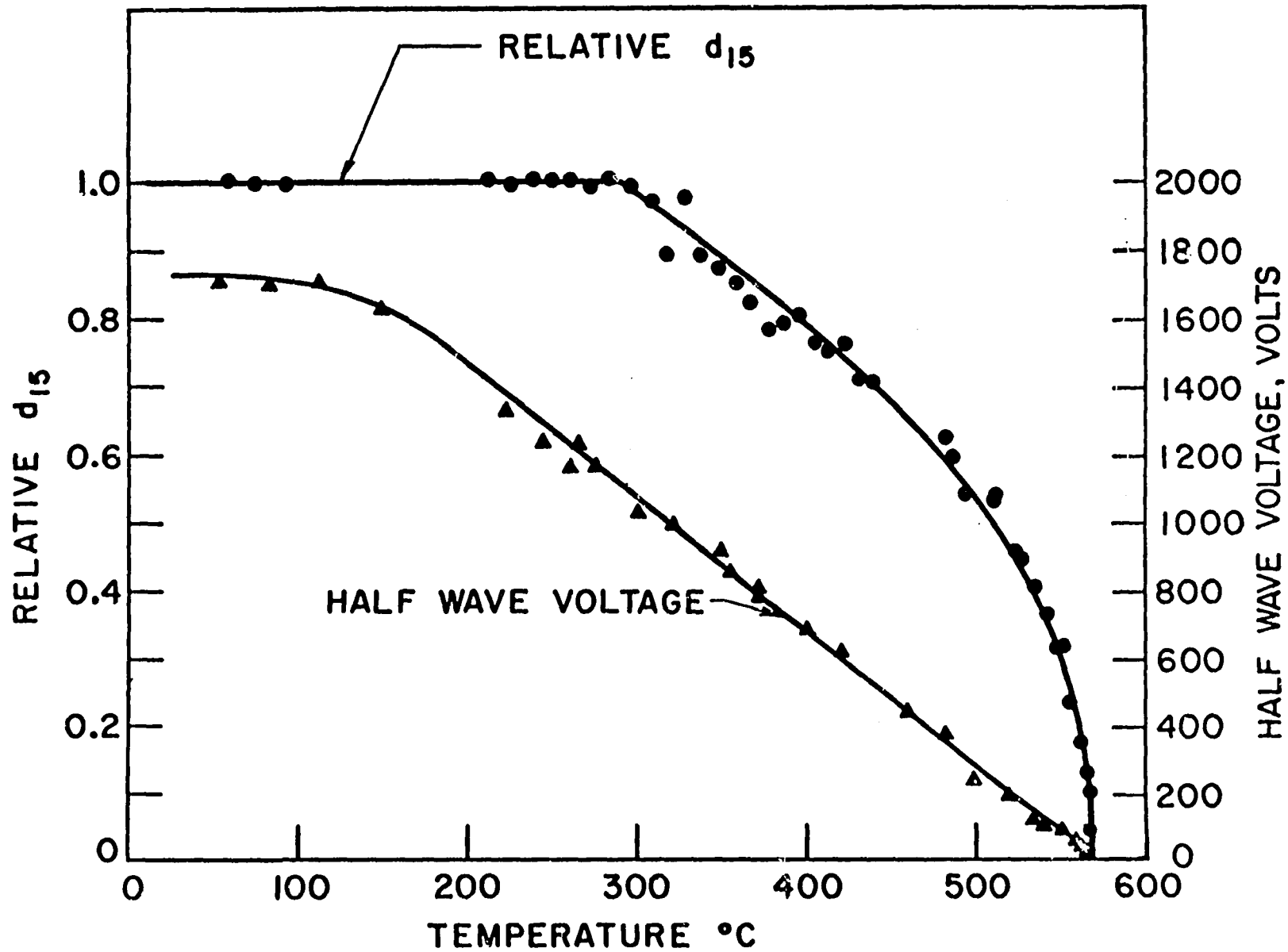

FIG. 7--Optical nonlinearity and half-wave voltage of barium sodium niobate as a function of crystal temperature.

Reproduced with permission of the copyright owner. Further reproduction prohibited without permission.

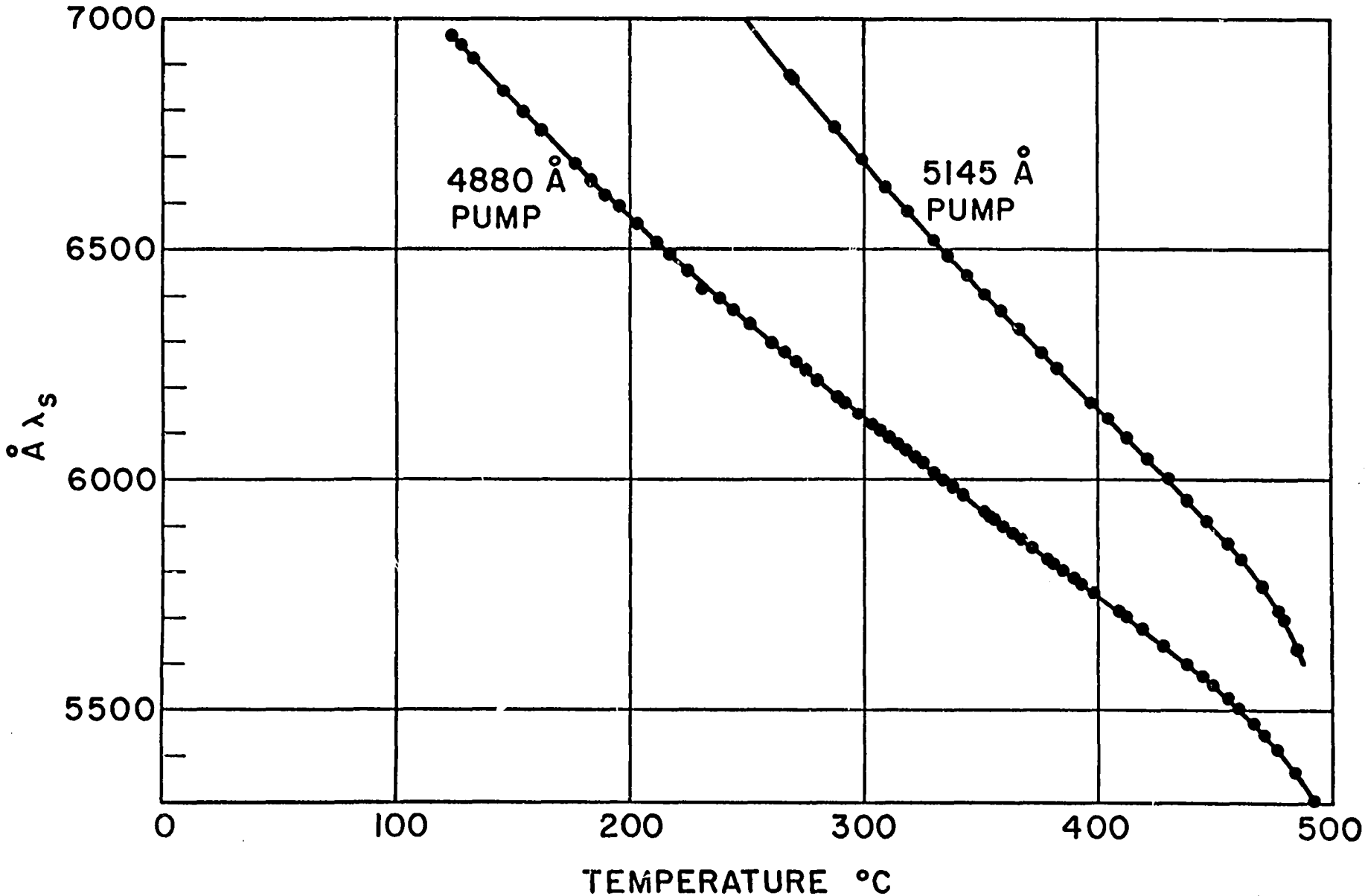

FIG. 8--Wavelength of spontaneous parametric emission of barium sodium niobate as a function of crystal temperature.

observing the wavelength of on-axis spontaneous parametric emission as a function of crystal temperature (19). The tuning curves are smooth and continuous through the phase transition at 300°C . The spontaneously emitted power decreases rapidly just below 500°C as the idler enters a region of high loss and rapidly increasing dispersion. Extrapolation from these curves indicates that the visible portion of the tuning curve for a doubled Nd:YAG pump would lie in the tetragonal-phase temperature range for 90° phase matching.

Calculations indicate that it should be possible to electro-optically tune (37) an optical parametric oscillator about 1000 cm^{-1} by using $Ba_2NaNb_5O_{15}$ at a temperature of 550°C , where the half-wave voltage is about 100 V and the optical nonlinearity is still reasonably large. However, as a result of the low resistivity (about 1.5 MΩ·cm) at these temperatures, such tuning could probably be achieved only on a repetitively pulsed basis if excessive crystal heating is to be avoided.

It should be noted that the $Ba_2NaNb_5O_{15}$ crystals were striated and remained so over the full temperature range examined. However, above 300°C a significant reduction of crystal strain was observed. The stria appear to consist of periodic variations of the index of refraction spaced ~ 15μ apart, and produce very large scattering losses. Attempts to remove the stria by adjusting growth parameters, varying melt composition, and annealing crystals in a controlled atmosphere were unsuccessful. In building his oscillator, Smith was able to find small areas where he could operate at low loss,

Reproduced with permission of the copyright owner. Further reproduction prohibited without permission.

apparently by squeezing the tightly focused mode between the stria. Despite his success we were concerned about the effect of placing such a crystal inside an argon ion laser, and a preliminary experiment was undertaken.

Experimental Results

An argon ion laser was constructed with a resonator structure of the general form shown in Fig. 5. The plasma tube was located between the flat and the lens. The mirrors were highly reflecting at 5145 Å , and the lens was antireflection coated. Cavity component positions were adjusted to provide a 20μ focus at the crystal position, while filling the 2 mm bore plasma tube. With no crystal, a circulating power at 5145 Å of about 19 watts was measured. We felt that this was reasonable and indicated a low loss cavity, considering that the plasma tube used provided an output of only 0.75 watts under normal conditions.

Two barium sodium niobate crystals were antireflection coated at 5145 Å for testing: a c-axis grown crystal 6 mm long along the a-axis; and an a-axis grown crystal 4 mm long. Both had been poled and detwinned, but were striated, the stria forming planes perpendicular to the growth direction. Each crystal was placed at the focal point of the cavity so that propagation was along the a-axis. The circulating power of the laser was measured for ordinary and extraordinary polarization orientations, and with the crystals at room temperature and heated above the transition temperature. In all cases the results

Reproduced with permission of the copyright owner. Further reproduction prohibited without permission.

were the same: the laser operated just above threshold with circulating powers of 1 to 2 watts at 5145 Å . A 50 to 1 chopper inside the cavity established that thermal focusing was not responsible for the effect, and despite lengthy experimentation with cavity parameters and crystal position no improvement could be made. The crystals seemed to introduce much more bulk loss, scattering, and mode distortion than expected from previous measurements. Evidently the crystal's mode distortions and loss were more damaging inside the resonator due to the many passes through the crystal.

Clearly, the quality of barium sodium niobate must be greatly improved, or a new material developed, before a cw SRO will be feasible. The techniques developed for $LiNbO_3$ and described in Chapter II are being applied to barium sodium niobate, but with little success to date.

Reproduced with permission of the copyright owner. Further reproduction prohibited without permission.

CHAPTER V

A CW RING CAVITY PARAMETRIC OSCILLATOR

When it became clear that a cw SRO was not feasible, we considered various schemes for reducing the undesirable properties of the DRO discussed in Chapter III. It appeared that an oscillator using a three mirror ring cavity would have two advantages over a more conventional two mirror linear cavity.

In the traveling wave ring cavity the resonating signal and idler waves do not travel through the crystal in the backward direction and there is, therefore, no parametrically generated backward pump wave. Recently Bjorkholm (38) pointed out that a parametric oscillator operating without a back generated pump wave has the potential of 100% conversion efficiency when operated four times above threshold, in contrast to a maximum of 50% for the linear cavity oscillator. In addition, the off-angle ring configuration provides very effective isolation between the oscillator and the pumping laser. The elimination of the back generated pump wave and of direct specular reflections from oscillator component surfaces should result in improved pump and oscillator stability. We therefore built the first ring cavity parametric oscillator to test these predictions and to determine if the improved characteristics justified the added complexity of a third mirror.

Reproduced with permission of the copyright owner. Further reproduction prohibited without permission.

Figure 9 shows the components of the ring cavity oscillator. Both the signal and idler waves were resonated in a three mirror cavity consisting of two 5 cm radius dielectric mirrors and a flat gold mirror. The nonlinear element was a 34 mm crystal of $LiNbO_3$ grown and tested as described in Chapter II. In contrast to the oscillator described in Chapter III, only a single longitudinal mode of the pump was effective in reaching threshold. A quartz etalon inside the laser resonator was used to select a single mode of the 5145 Å argon ion laser. The pump was continuously monitored with a confocal scanning Fabry-Perot interferometer to ensure that it was single frequency. Operation was far from degenerate with a tuning range from 6600 Å to 7000 Å at the signal and a corresponding idler tuning range near 2.0μ . A three-to-one ratio of signal-to-idler frequencies was again chosen to simplify the fabrication of the 5 cm dielectric mirrors and the $LiNbO_3$ antireflection coatings. The gold coated flat mirror was mounted just above the crystal inside the oven so that the dielectric mirrors were used at nearly normal incidence. Alignment was accomplished using the pump beam and the small reflectivity of the oscillator components at 5145 Å . We were surprised to find that the three mirror cavity was not significantly harder to align than a two mirror cavity. The oscillator could be constructed in as short a time as one hour, although if difficulties were encountered the better part of a day might be needed. The experience and techniques gained from the first oscillator proved extremely valuable during this experiment.

Reproduced with permission of the copyright owner. Further reproduction prohibited without permission.

Reproduced with permission of the copyright owner. Further reproduction prohibited without permission.

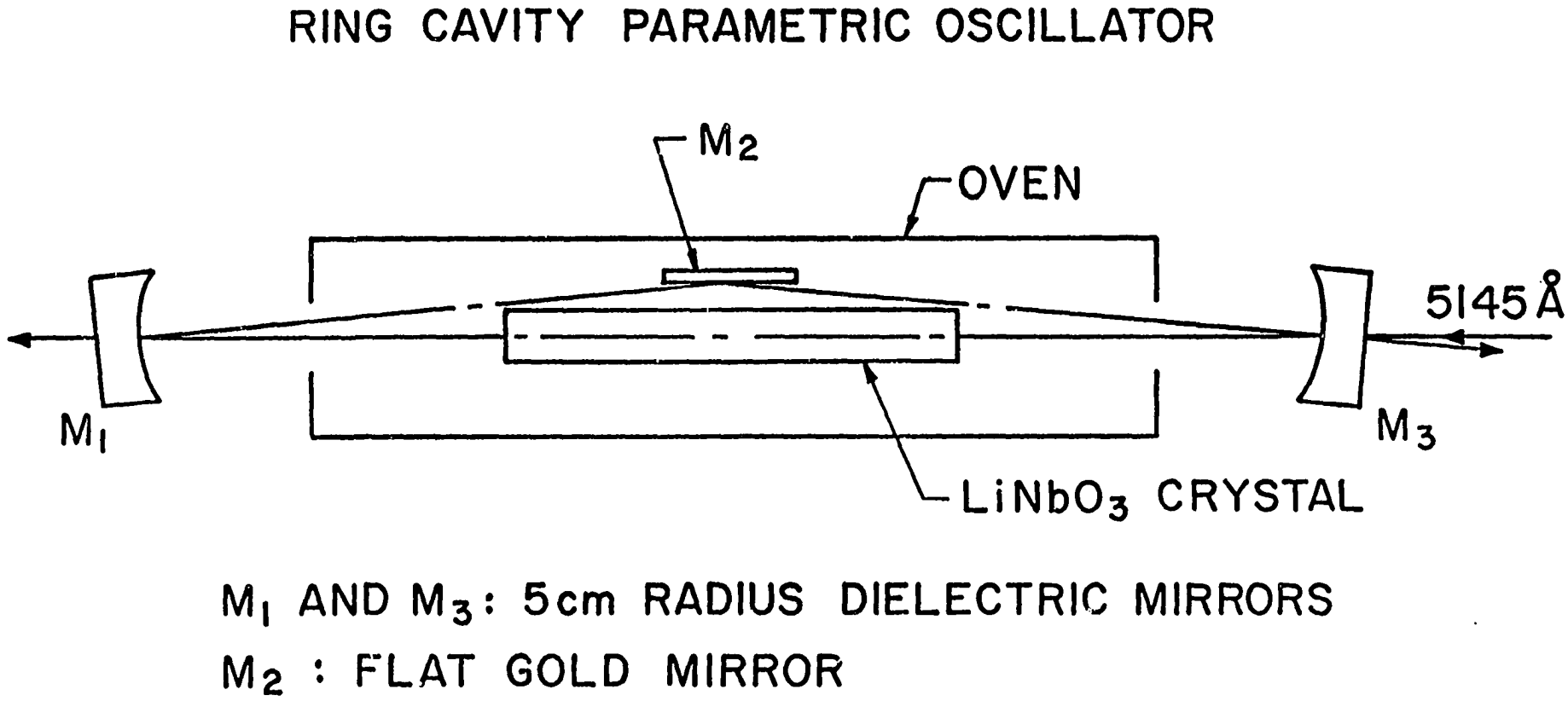

FIG. 9--Schematic of the ring cavity optical parametric oscillator.

The single-pass cavity loss at the signal and idler was approximately 2% each which, with the confocal mode radii of 40μ and 70μ at the signal and idler respectively, gives a theoretical threshold of 50 mW . Initially, a conventional linear cavity oscillator was constructed using the 34 mm crystal and the two 5 cm radius mirrors. A 60 mW threshold indicated that the alignment techniques were good and the estimated cavity losses correct. The ring cavity oscillator, however, had a threshold of 150 mW . We believe that this increase was due primarily to the added loss of the gold flat used at grazing incidence inside the oven. The gold flat also seemed to be effected by the heat of the oven, since the threshold increased slowly during operation, but could be reduced by replacing the gold flat. It is also probable that at least some of the discrepancy between calculated and observed threshold values resulted from an imcomplete overlap of the pump, signal, and idler waves in the crystal, as a consequence of the more difficult alignment problem.

We observed up to 60% pump depletion indicating operation near two times above threshold. Operation further above threshold was not possible due to limited pump power. No precautions were taken to stabilize the oscillator or pump cavities and the erratic behavior typical of doubly resonant oscillators was observed. However, the ring cavity oscillator exhibited on-times as much as ten times longer than the linear cavity oscillator constructed using the same components. The Fabry-Perot interferometer clearly showed the greatly improved frequency stability of the pump due to the effective isolation of the ring cavity configuration. In spite of the large pump depletion

Reproduced with permission of the copyright owner. Further reproduction prohibited without permission.

the output power at the signal was relatively low due to the large ratio of internal losses to coupling losses, and peak output powers at the signal of only a few milliwatts were observed. Improvements in the output coupling should lead to the expected highly efficient operation.

In conclusion, the operation of this parametric oscillator verified the increased pump depletion predicted for a parametric oscillator operating without the back generated pump wave, and also showed the improved stability which can result from the optical isolation afforded by the ring cavity configuration.

Reproduced with permission of the copyright owner. Further reproduction prohibited without permission.

CHAPTER VI

CONCLUSIONS

The oscillators described in this report represent the first step in the development of truely useful cw tunable optical sources. Optical techniques play an important role in many areas of science and engineering, and the development of tunable coherent sources is certain to receive considerable effort and support. These initial experiments have created the interest and provided the techniques and confidence necessary for further advancements.

It has become clear in the course of this work that the most critical component of parametric oscillators is the nonlinear material. Material properties determine all the meaningful device parameters: gain, bandwidth, and tuning range. In addition, crystal quality requirements for effective nonlinear interactions are much more severe than for previous applications. Suitable high quality lithium niobate crystals are now available, but barium sodium niobate still needs much development. Clearly, the development, and even design of materials having desirable characteristics will continue to be an essential part of research in nonlinear optical devices.

Reproduced with permission of the copyright owner. Further reproduction prohibited without permission.

LIST OF REFERENCES

1. R. L. Byer, M. K. Oshman, J. F. Young, and S. E. Harris, "Visible CW Parametric Oscillator," Appl. Phys. Letters 13, 109 (August 1968).
2. R. L. Byer, S. E. Harris, D. J. Kuizenga, R. S. Feigelson, and J. F. Young, "Nonlinear Optical Properties of $Ba_2NaNb_5O_{15}$ in the Tetragonal Phase," J. Appl. Phys. 40, 444 (January 1969).
3. R. L. Byer, A. Kovrigin, and J. F. Young, "A CW Ring Cavity Parametric Oscillator," Appl. Phys. Letters 15, 136 (September 1969).
4. R. L. Byer and J. F. Young, "Growth of High Quality Lithium Niobate Crystals from the Congruent Melt," to be published.
5. S. E. Harris, "Tunable Optical Parametric Oscillators," to be published in Proc. IEEE.
6. R. J. Collins, D. F. Nelson, A. L. Schawlow, W. Bond, G. G. B. Garrett, and W. Kaiser, "Coherence, Narrowing, Directionality, and Relaxation Oscillations in the Light Emission from Ruby," Phys. Rev. Letters 5, 303 (October 1960).
7. W. H. Louisell, Coupled Mode and Parametric Electronics (John Wiley and Sons, Inc., New York), 1960.
8. R. H. Kingston, "Parametric Amplification and Oscillation at Optical Frequencies," Proc. IRE 50, 472 (April 1962).

Reproduced with permission of the copyright owner. Further reproduction prohibited without permission.

9. N. M. Kroll, "Parametric Amplification in Spatially Extended Media and Application to the Design of Tunable Oscillators at Optical Frequencies," Phys. Rev. 127, 1207 (August 1962).

10. S. A. Akhmanov and R. V. Khokhlov, "Concerning One Possibility of Amplification of Light Waves," JETP 16, 252 (January 1963).

11. R. W. Minck, R. W. Terhune, and C. C. Wang, "Nonlinear Optics," Appl. Optics 5, 1595 (October 1966).

12. P. A. Franken, A. E. Hill, C. W. Peters, and G. Weinreich, "Generation of Optical Harmonics," Phys. Rev. Letters 7, 118 (August 1961).

13. J. A. Giordmaine and R. C. Miller, "Tunable Coherent Parametric Oscillation in $LiNbO_3$ at Optical Frequencies," Phys. Rev. Letters 14, 973 (June 1965).

14. G. D. Boyd, R. C. Miller, K. Nassau, W. L. Bond, and A. Savage, "$LiNbO_3$: An Efficient Phase-Matchable Nonlinear Optical Material," Appl. Phys. Letters 5, 234 (December 1964).

15. G. D. Boyd and A. Ashkin, "Theory of Parametric Oscillator Threshold with Single-Mode Optical Masers and Observation of Amplification in $LiNbO_3$," Phys. Rev. 146, 187 (June 1966).

16. R. G. Smith, J. E. Geusic, H. J. Levinstein, J. J. Rubin, S. Singh, and L. G. Van Uitert, "Continuous Optical Parametric Oscillation in $Ba_2NaNb_5O_{15}$," Appl. Phys. Letters 12, 308 (May 1968).

17. J. A. Giordmaine, "Mixing of Light Beams in Crystals," Phys. Rev. Letters 8, 19 (January 1962).

Reproduced with permission of the copyright owner. Further reproduction prohibited without permission.

18. S. E. Harris, M. K. Oshman, and R. L. Byer, "Observation of Tunable Optical Parametric Fluorescence," Phys. Rev. Letters 18, 732 (May 1967).

19. R. L. Byer and S. E. Harris, "Power and Bandwidth of Spontaneous Parametric Emission," Phys. Rev. 168, 1064 (April 1968).

20. M. K. Oshman, "Studies of Optical Frequency Parametric Oscillation," Stanford University Microwave Laboratory Report No. 1602 (December 1967).

21. J. E. Midwinter, "Assessment of Lithium-Meta-Niobate for Nonlinear Optics," Appl. Phys. Letters 11, 128 (August 1967).

22. J. E. Midwinter, "Lithium Niobate: Effects of Composition on the Refractive Indices and Optical Second Harmonic Generation," J. Appl. Phys. 39, 3033 (June 1968).

23. Homer Fay, W. J. Alford, and H. M. Dess, "Dependence of Second-Harmonic Phase-Matching Temperature in $LiNbO_3$ Crystals on Melt Composition," Appl. Phys. Letters 12, 89 (February 1968).

24. J. G. Bergman, A. Ashkin, A. A. Ballman, J. M. Dziedzic, H. J. Levinstein, and R. G. Smith, "Curie Temperature, Birefringence, and Phase-Matching Temperature Variations in $LiNbO_3$ as a Function of Melt Stoichiometry," Appl. Phys. Letters 12, 92 (February 1968).

25. A. Ashkin, G. D. Boyd, J. M. Dziedzic, R. G. Smith, A. A. Ballman, H. J. Levinstein, and K. Nassau, "Optically-Induced Refractive Index Inhomogeneities in $LiNbO_3$ and $LiTaO_3$," Appl. Phys. Letters 9, 72 (July 1966).

Reproduced with permission of the copyright owner. Further reproduction prohibited without permission.

26. P. Lerner, C. Legras, and J. P. Dumas, "Stoechiometre des Monocristaux de Metaniobate de Lithium," J. Crystal Growth 3, 231 (April 1968).

27. A. Reisman and F. Holtzberg, "Heterogeneous Equilibria in the Systems Li_2O - Ag_2O - Nb_2O_5 and Oxide-Models," J. Amer. Chem. Soc. 80, 6503 (December 1958).

28. M. V. Hobden and J. Warner, "The Temperature Dependence of the Refractive Indices of Pure Lithium Niobate," Phys. Letters 22, 243 (August 1966).

29. M. K. Oshman and S. E. Harris, "Theory of Optical Parametric Oscillation Internal to the Laser Cavity," J. Quant. Elect. QE-4, 491 (August 1968).

30. S. E. Harris, "Threshold of Phase Locked Parametric Oscillators," J. Quant. Elect. QE-3, 205 (May 1967).

31. S. E. Harris, "Threshold of Multimode Parametric Oscillators," J. Quant. Elect. QE-2, 701 (October 1966).

32. A. E. Siegman, "Nonlinear Optical Effects: An Optical Power Limiter," Appl. Optics 1, 739 (November 1962).

33. J. F. Young, "A Computer Program to Analyze Optical Resonators," Stanford University Microwave Laboratory Report No. 1803 (November 1969).

34. H. Kogelnik and T. Li, "Laser Beams and Resonators," Appl. Optics 5, 1550 (October 1966).

Reproduced with permission of the copyright owner. Further reproduction prohibited without permission.

35. J. E. Geusic, H. J. Levinstein, J. J. Rubin, S. Singh, and L. G. Van Uitert, "The Nonlinear Optical Properties of $Ba_2NaNb_5O_{15}$," Appl. Phys. Letters 11, 219 (November 1967).

36. S. Singh, D. A. Draegert, J. E. Geusic, H. J. Levinstein, R. G. Smith, and L. G. Van Uitert, 1968 International Quantum Electronics Conference, Miami, Florida (May 13-17, 1968).

37. L. B. Kreuzer, "Ruby-Laser-Pumped Optical Parametric Oscillator with Electro-Optic Effect Tuning," Appl. Phys. Letters 10, 336 (June 1967).

38. J. E. Bjorkholm, "Analysis of the Doubly Resonant Optical Parametric Oscillator Without Power-Dependent Reflections," J. Quant. Elect. QE-5, 293 (June 1969).

Reproduced with permission of the copyright owner. Further reproduction prohibited without permission.